# Selective Colorimetric Detection of Polynucleotides Based on the Distance-Dependent Optical Properties of Gold Nanoparticles

Robert Elghanian *et al.*

*Science* **277**, 1078 (1997);
DOI: 10.1126/science.277.5329.1078

# Selective Colorimetric Detection of Polynucleotides Based on the Distance-Dependent Optical Properties of Gold Nanoparticles

Robert Elghanian, James J. Storhoff, Robert C. Mucic, Robert L. Letsinger,* Chad A. Mirkin*

A highly selective, colorimetric polynucleotide detection method based on mercaptoalkyloligonucleotide-modified gold nanoparticle probes is reported. Introduction of a single-stranded target oligonucleotide (30 bases) into a solution containing the appropriate probes resulted in the formation of a polymeric network of nanoparticles with a concomitant red-to-pinkish/purple color change. Hybridization was facilitated by freezing and thawing of the solutions, and the denaturation of these hybrid materials showed transition temperatures over a narrow range that allowed differentiation of a variety of imperfect targets. Transfer of the hybridization mixture to a reverse-phase silica plate resulted in a blue color upon drying that could be detected visually. The unoptimized system can detect about 10 femtomoles of an oligonucleotide.

Sequence-specific methods for detecting polynucleotides are critical to the diagnosis of genetic and pathogenic diseases (*1*). Most detection systems make use of the hybridization of an immobilized target polynucleotide with oligo- or polynucleotide probes containing covalently linked reporter groups (*2*–*5*). Radioactive $^{32}P$ or $^{35}S$ labels in polynucleotide detection offer exquisite sensitivity and are commonly used to follow hybridization (*3*). However, radioactive probes create disposal problems, require specially trained personnel, and have a short shelf life. Increasingly, radioactive atoms are being replaced by nonradioactive organic reporter groups, which are detected by their color, fluorescence, or luminescence (*2*, *3*, *5*). The organic groups may either be covalently attached to the probes or may be generated in solution by enzymes that are bound to the probe. Each of these strategies has advantages and disadvantages, depending on the target DNA molecules and detection environments, and no single method has gained supremacy (*2*).

Herein, we report a highly selective colorimetric detection technology for polynucleotides that differs fundamentally from previously described sensor systems in several respects. First, mercaptoalkyloligonucleotide-modified Au nanoparticles are used as reporter groups rather than radioactive atoms or organic substituents. Second, hybridization results not only in the binding of an oligonucleotide probe to the target sequence, but also in the formation of an extended polymeric network in which the reporter units are interlocked by multiple, short duplex segments (Fig. 1). Third, the signal for hybridization is governed by the optical properties of the nanoparticles, which depend in part on their spacing within the polymeric aggregate. Nanoparticle aggregates with interparticle distances substantially greater than the average particle diameter appear red, but as the interparticle distances in these aggregates decrease to less than approximately the average particle diameter, the color becomes blue (*6*). This shift, attributed to the surface plasmon resonance of the Au, has been observed in other non–oligonucleotide-based strategies for organizing nanoparticles into aggregate structures (*7*) and has been studied theoretically (*8*). Gold particles ~13 nm in diameter (*9*) were chosen because they can be readily prepared with little deviation in size (±2 nm) and exhibit a sharp plasmon absorption band (maximum absorbance at wavelength 520 nm). Two additional factors proved helpful in developing this technology: (i) hybridization is greatly accelerated by heating or freezing the solutions and (ii) the color changes associated with hybridization are significantly enhanced and easily visualized if the hybridized sample is "developed" on a solid support. With these techniques, target polynucleotides can be identified rapidly without instrumentation.

The use of mercaptoalkyloligonucleotide-modified Au nanoparticles in any sensing scheme requires that they exhibit long-term stability in the presence of high molecular weight DNA and in solutions that span a wide range of electrolyte concentration (0.1 to 1 M NaCl). The nanoparticles previously used in our material syntheses strategies (*10*) do not exhibit this type of long-term environmental stability. However, with the current preparation procedure, one can synthesize Au nanoparticles modified with oligonucleotide of variable length and sequence that exhibit long-term stability in 1 M NaCl solutions and in solutions containing macromolecular salmon sperm DNA (up to 100 μg of salmon sperm DNA can be added to a solution containing 50 μl of each probe prepared without interfering with the sensor applications). In our protocol, nanoparticles are loaded with 5′- or 3′-mercaptoalkyloligonucleotides in solution without added salt, aged in 0.1 M NaCl for 40 hours in the presence of the mercaptoalkyloligonucleotides to increase the loading, collected by centrifugation, and resuspended. This procedure was used to prepare all of the nanoparticle probes described herein.

Initial studies were carried out with a three-component system, wherein two probes, **1** and **2**, were used for one target sequence, **3** (Fig. 2A). Each nanoparticle has many molecules of a 28-base oligomer linked by a thiol tether at the 5′ terminus to its surface (*11*). The first 13 nucleotides (not shown) of the 28-base oligomers serve as a flexible spacer (*12*), and the last 15 serve as a recognition element for the target. Sequences were selected such that on hybridization, the recognition segments of probes **1** and **2** could align contiguously on the target **3**.

For this system, hybridization was slow when the components (probes and target) (*13*) stood in 0.1 M NaCl at room temperature, but after standing overnight, the solution changed from red to reddish purple. The slow rate of the reaction may be due to steric considerations and the high negative charge density created by the extensive oligonucleotide loading on the nanoparticle surfaces. A similar color change could be

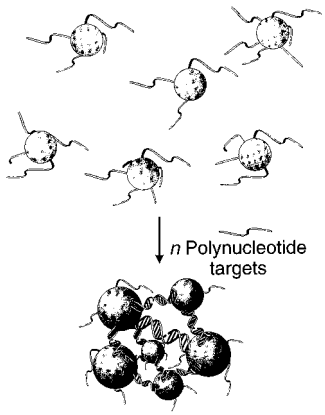


**Fig. 1.** Schematic representation of the concept for generating aggregates signaling hybridization of nanoparticle-oligonucleotide conjugates with oligonucleotide target molecules. The nanoparticles and the oligonucleotide interconnects are not drawn to scale, and the number of oligomers per particle is believed to be much larger than depicted.

Department of Chemistry, Northwestern University, Evanston, IL 60208, USA.

*To whom correspondence should be addressed. E-mail: camirkin@chem.nwu.edu and r-letsinger@chem.nwu.edu

effected rapidly, however, by warming the mixture at 50°C for 5 min or freezing it in a bath of dry ice and isopropyl alcohol and then thawing it at room temperature. The acceleration in rate caused by freezing likely reflects the development of high local concentrations of salt, the oligonucleotide target, and nanoparticles within pockets in the ice structure (*14*). Control experiments showed that the transition requires the presence of all three components (both types of nanoparticle conjugates and the target oligonucleotide), and in absence of hybridization, the probes are not affected by the process, as evidenced by ultraviolet-visible spectroscopy and transmission electron microscopy.

A "melting curve" obtained at a wavelength of 260 nm on a nanoparticle-DNA aggregate hybridized by the freeze-thaw cycle gave a "melting" temperature ($T_m$) of 57°C (Fig. 3A, black circles), as compared with $T_m$ = 56°C for a solution of free oligonucleotides hybridized in solution at room temperature in the absence of nanoparticles (Fig. 3A, red squares). The curve for the Au-nanoparticle/DNA complex is remarkably steep; the temperature range for melting [full width at half maximum (FWHM) = 4°C] is narrow compared with the temperature range for dissociation of the complex formed from the free oligonucleotides (FWHM = 12°C) [Fig. 3A, insets (*15*)]. Corresponding sharp transitions at the same temperature but with a drop in absorbance rather than an increase were obtained when the dissociation of the nanoparticle aggregates was observed at 620 and 700 nm. All of the experiments with the nanoparticle conjugates measure changes in the optical properties of the nanoparticles (not the DNA). The oligonucleotides do not absorb at 620 and 700 nm, and the concentration of the target oligonucleotide in the colloid solution is too low to account for the absorbance change at 260 nm.

We attribute the spectral changes in this nanoparticle system to the reversible formation and dissociation of aggregates formed by hybridization of the covalently attached probe segments with the target oligonucleotide. Hybridization results in decreased interparticle distances with a concomitant change in color and formation of extended polymeric nanoparticle aggregates (*16*). On warming, some of the DNA cross-links can dissociate without dispersing the Au nanoparticles into solution. Because the signal depends on the nanoparticle spacing, our melting analysis is insensitive to these initial DNA dissociation events, and the observed temperature range for "melting" is unusually narrow. The size of the aggregates in these systems may also influence the colorimetric change, but this issue has not yet been addressed.

A simpler way to monitor hybridization is to spot 1 to 3 μl of the solution containing the Au-nanoparticle/DNA aggregates on a $C_{18}$ thin-layer chromatography (TLC) plate (Fig. 3B). Initially, the spot retains the color of the solution mixture, which ranges from red in the absence of hybridization through reddish-purple to purple on hybridization, depending on the system. On drying, a uniform blue spot develops if the Au-oligonucleotide conjugates have been linked by hybridization with the target oligonucleotide; in the absence of an appropriate target or with solutions spotted above thermal denaturation conditions, the spot remains pink. The color differentiation is enhanced by the $C_{18}$-silica support, a phenomenon at-

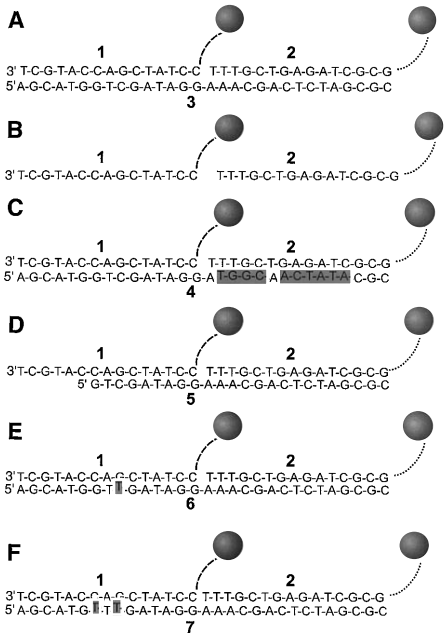


**Fig. 2.** Mercaptoalkyloligonucleotide-modified 13-nm Au particles and polynucleotide targets used for examining the selectivity of the nanoparticle-based colorimetric polynucleotide detection system. (**A**) Complementary target; (**B**) probes without the target; (**C**) a half-complementary target; (**D**) a 6-bp deletion; (**E**) a 1-bp mismatch; and (**F**) a 2-bp mismatch. For the sake of clarity, only two particles are shown; in reality a polymeric aggregate with many particles is formed. Dashed lines represent flexible spacer portions of the mercaptoalkyloligonucleotide strands bound to the nanoparticles; note that these spacers, because of their noncomplementary nature, do not participate in hybridization. The full sequences for the two probes, **1** and **2**, which bind to targets **3** through **7**, are

**1**-5′SH-$(CH_2)_6$- [CTA-ATC-CGC-ACA-G]
spacer

[CC-TAT-CGA-CCA-TGC-T]
probe

**2**-5′SH-$(CH_2)_6$-[ATG-GCA-ACT-ATA-C]
spacer

[GC-GCT-AGA-GTC-GTT-T]
probe

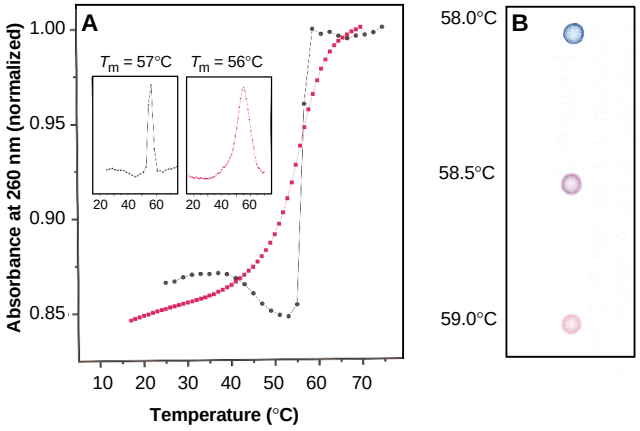


**Fig. 3.** (**A**) Comparison of the thermal dissociation curves for complexes of mercaptoalkyloligonucleotide-modified Au nanoparticles (black circles) and mercaptoalkyloligonucleotides without Au nanoparticles (red squares) with the complementary target, **3**, in hybridization buffer (0.1 M NaCl, 10 mM phosphate buffer, pH 7.0). For the first set (black circles), a mixture of 150 μl of each colloid conjugate and 3 μl of the target oligonucleotide in hybridization buffer (0.1 M NaCl, 10 mM phosphate, pH 7.0) was frozen at the temperature of dry ice, kept for 5 min, thawed over a period of 15 min, and diluted to 1.0 ml with buffer (final target concentration, 0.02 μM). The absorbance was measured at 1-min intervals with a temperature increase of 1°C per minute. The increase in absorption at 260 nm ($A_{260}$) was ~0.3 absorption units (AU). In the absence of the oligonucleotide targets, the absorbance of the nanoparticles did not increase with increasing temperature. For the second set, the mercaptoalkyloligonucleotides and complementary target (each 0.33 μM) were equilibrated at room temperature in 1 ml of buffer, and the changes in absorbance with temperature were monitored as before. The increase in $A_{260}$ was 0.08 AU. (**Insets**) Derivative curves for each set (*15*). (**B**) Spot test showing $T_c$ (thermal transition associated with the color change) for the Au nanoparticle probes hybridized with complementary target. A solution prepared from 150 μl of each probe and 3 μl of the target (0.06 μM final target concentration) was frozen for 5 min, allowed to thaw for 10 min, transferred to a 1-ml cuvette, and warmed at 58°C for 5 min in the thermally regulated cuvette chamber of the spectrophotometer. Samples (3 μl) were transferred to a $C_{18}$ reverse phase plate with an Eppendorf pipette as the temperature of the solution was increased incrementally 0.5°C at 5-min intervals.

tributable to increased aggregation of the preorganized polynucleotide-linked nanoparticles upon drying the solution on the support. Moreover, the solid support prevents samples heated above the DNA dissociation temperature from rehybridizing; therefore, the colors are indefinitely stable, and the plates provide a permanent record of the test.

A striking feature of this test is the sharpness and clarity of the transition (Fig. 3B). The spot was blue for a hybridized sample containing **1**, **2**, and **3** heated in solution to 58°C before the test, indicating that the nanoparticles were still assembled at this temperature. However, the spot was pink when the sample was heated to 59°C, a temperature at which the assembly is unstable and the nanoparticles are dispersed in solution. At 58.5°C, the color was intermediate. We term this the colorimetric temperature $T_c$, which is close to but slightly higher than $T_m$ (57°C) for the polymeric aggregate, as determined by the change in the ultraviolet spectrum for the solution (Fig. 3A). Repetitions of the spot test with another set of probes prepared independently afforded the same narrow range for the color change with $T_c$ = 58.0°C.

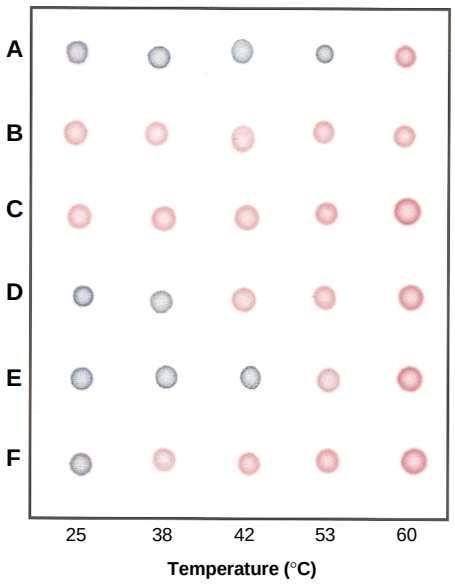


**Fig. 4.** Selective polynucleotide detection for the target probes shown in Fig. 2: (**A**) complementary target; (**B**) no target; (**C**) complementary to one probe; (**D**) a 6-bp deletion; (**E**) a 1-bp mismatch; and (**F**) a 2-bp mismatch. Nanoparticle aggregates were prepared in a 600-μl thin-walled Eppendorf tube by addition of 1 μl of a 6.6 μM oligonucleotide target to a mixture containing 50 μl of each probe (0.06 μM final target concentration). The mixture was frozen (5 min) in a bath of dry ice and isopropyl alcohol and allowed to warm to room temperature. Samples were then transferred to a temperature-controlled water bath, and 3-μl aliquots were removed at the indicated temperatures and spotted on a $C_{18}$ reverse phase plate.

The small temperature range for the change in color enables one to discriminate between the perfect complement (**3**) and the mismatched targets (**4** to **7**) (Figs. 2 and 4). In each test, the probe-target mixtures were frozen, thawed at room temperature, warmed in a water bath at the indicated temperature for 5 min, and then spotted on a $C_{18}$-silica plate. At 53°C, the test was positive (blue) for the fully matched target (Figs. 2A and 4A) but negative (pink) for the target with one mismatched base (Figs. 2E and 4E). At 42°C, it was positive for the target with one mismatched base (Figs. 2E and 4E) but negative for targets with two mismatches (Figs. 2F and 4F) or a six-base deletion (Figs. 2D and 4D). As expected, tests with the target absent (Figs. 2B and 4B) or with extensive mismatches in the segment targeted by one of the probes (Figs. 2C and 4C) were negative.

This system of nanoparticles, aggregates, and oligonucleotides is complex. At this stage we treat these colorimetric transition temperatures as empirical values useful in detecting and differentiating oligonucleotides with specific sequences. To examine the dependence of the results on the hybridization procedure, we, rather than freezing the solutions, warmed individual samples of targets **3** through **7** with solutions containing **1** and **2** to 65°C (a temperature above the dissociation temperatures of the complex formed with the fully matched target) and allowed the solutions to cool slowly with intermittent pauses of 5 min at 62°, 53°, 42°, 38°, and 25°C. At the end of each pause, the samples were removed and spotted as before. The plate obtained by this procedure was identical to that in Fig. 4, except that **7** gave a blue rather than pink spot at 38°C (when spotted at 39.5°C, however, the color was pink, indicative of dissociation). This experiment shows that there is considerable latitude in conditions for carrying out the assays, although the absolute $T_c$ values may vary slightly with changes in the method for hybridization.

The high degree of discrimination in these systems may be attributed to two features. (i) Alignment of two relatively short (15 nucleotide) probe oligonucleotides on the target is required for a positive signal (Figs. 2C and 4C). A mismatch in either segment is more destabilizing than a mismatch for a single, longer probe (such as a 30-nucleotide segment) with the same target. (ii) As in the spectrophotometric analyses, the colorimetric signal depends on the formation or dissociation of a polymeric network of Au nanoparticles held together by multiple structurally similar tethers (that is, the oligonucleotide duplexes), which results in the narrowing of the temperature range observed for the transition. In principle, this three-component nanoparticle-based strategy should be more selective than any two-component detection system based on a single-strand probe hybridizing with the target. Strategies such as ours that exploit reversible assembly of particles by hybridization and use probes with signals sensitive to particle aggregation or distance should prove generally useful in designing highly discriminating nucleic acid detection systems. We do not yet know the ultimate sensitivity of the system, although with the unoptimized system, ~10 fmol of an oligonucleotide can be detected (*17*). The method should be particularly useful in assays where expense and simplicity in instrumentation and operation are important.

## REFERENCES AND NOTES


1. S. Razin, *Mol. Cell. Probes* **8**, 497 (1994); J. G. Hacia *et al.*, *Nature Genet.* **14**, 441 (1996).
2. E. S. Mansfield *et al.*, *Mol. Cell. Probes* **9**, 145 (1995); L. J. Kricka, Ed., *Nonisotopic DNA Probe Techniques* (Academic Press, San Diego, 1992).
3. B. D. Hames and S. J. Higgins, Eds., *Gene Probes 1* (IRL Press, New York, 1995).
4. J. Wang *et al.*, *J. Am. Chem. Soc.* **118**, 7667 (1996).
5. S. Tyagi and F. R. Kramer, *Nature Biotechnol.* **14**, 303 (1996).
6. U. Kreibig and L. Genzel, *Surf. Sci.* **156**, 678 (1985); B. Dusemund *et al.*, *Z. Phys. D* **20**, 305 (1991).
7. M. Brust *et al.*, *Adv. Mater.* **7**, 795 (1995); K. C. Grabar *et al.*, *J. Am. Chem. Soc.* **118**, 1148 (1996); J. J. Storhoff, R. C. Mucic, C. A. Mirkin, *J. Cluster Sci.*, **8**, 179 (1997).
8. W.-H. Yang, G. C. Schatz, R. P. Van Duyne, *J. Chem. Phys.* **103**, 869 (1995).
9. K. C. Grabar *et al.*, *Anal. Chem.* **67**, 735 (1995); G. Frens, *Nature Phys. Sci.* **241**, 20 (1973).
10. C. A. Mirkin *et al.*, *Nature* **382**, 607 (1996).
11. Multiple loading of the oligonucleotides is necessary for subsequent cross-linking in our system. The surface chemistry involved in linking alkylthiols to Au surfaces is still a subject of debate [see C. S. Weisbecker *et al.*, *Langmuir* **12**, 3763 (1996)]. An alternative method of binding oligonucleotides covalently to Au particles, which was developed for a different purpose, was reported to give ~1-nm nanoparticles containing a single oligomer on a particle [A. P. Alivisatos *et al.*, *Nature* **382** 609 (1996)].
12. Subsequent experiments have shown that the oligonucleotide spacer is not essential.
13. The concentrations for the three components were the same as those described in the caption for Fig. 3A.
14. For another example in which the rate of a reaction dependent on the hybridization of oligonucleotides was accelerated by the freezing of an aqueous solution of the components, see S. M. Gryaznov and R. L. Letsinger, *J. Am. Chem. Soc.* **115**, 3808 (1993).
15. We calculated the temperature ranges for both melting analyses depicted in Fig. 3A by measuring the full width at half maximum for each derivative curve (Fig. 3A, insets). The value of $T_m$ for the nanoparticle system hybridized by the freeze-thaw method agreed (±0.2°C) with that for the nanoparticle system hybridized at room temperature (24 hours).
16. Transmission electron microscopy pictures of typical aggregates are available in supplementary material. Similar images can be found in (*10*).
17. For this experiment, 1 μl of solution containing 10 fmol of target oligonucleotide and 1 μl of solution containing both nanoparticle probes in a buffer (0.3

M NaCl, 10 mM phosphate, pH 7.0) were mixed, frozen (40 s), thawed (5 min), and spotted with a capillary tube on a $C_{18}$ TLC plate. A blue spot developed. In the absence of target, the color remained pink. For comparison, the lower limit for detecting an oligonucleotide with the use of a probe labeled with fluorescein in a sandwich hybridization system was reported to be 500 fmol [M. S. Urdea *et al.*, *Nucleic Acids Res.* **16**, 4937 (1988)].

18. We acknowledge support by grants from the National Institute of General Medical Sciences (GM 10265) and the Office of Naval Research (N0014-94-1-0703 and N00014-97-10430) and the Department of Defense (MURI DAAG 55-97-1-0133).

16 April 1997; accepted 24 June 1997

# Superconductivity up to 126 Kelvin in Interstitially Doped $Ba_2Ca_{n-1}Cu_nO_x$ [02(*n*–1)*n*–Ba]

C. W. Chu,* Y. Y. Xue, Z. L. Du, Y. Y. Sun, L. Gao, N. L. Wu,† Y. Cao, I. Rusakova, K. Ross

A new high-temperature superconducting compound system, $Ba_2Ca_{n-1}Cu_nO_x$ [02(*n*–1)*n*–Ba] interstitially doped with calcium or (Ca,Cu) has been identified to exhibit a transition temperature up to 126 kelvin, the highest for a superconductor without a volatile toxic element. 02(*n*–1)*n*–Ba has body-centered tetragonal symmetry and an unusual charge-reservoir block. The compounds offer interesting opportunities for high-temperature superconductivity science and technology.

In the past 10 years, many high-temperature layered cuprate superconductors have been discovered (*1*). They can be represented by the generic formula $A_mE_2R_{n-1}Cu_nO_{2n+m+2}$ with a stacking sequence of $m$ layers of (AO) inserted between two layers of (EO) on top of $n$ layers of ($CuO_2$) interleaved by ($n$–1) layers of (R), where A, E, and R are various cations. The generic formula may be abbreviated in terms of the four-digit classification scheme (*2*) *m*2(*n*–1)*n* or A-*m*2(*n*–1)*n*–E for further subclassification. Presently, all superconductors that have transition temperatures ($T_c$'s) above the liquid nitrogen boiling point of 77 K belong to or are derivable from the following compound families: (i) Cu-1212-Ba with R = Y or a rare-earth element, except Ce, Pr and Tb (such as $CuBa_2$ $YCu_2O_7$ = $YBa_2Cu_3O_7$, commonly known as Y-123); (ii) A-22(*n*–1)*n*–E with A = Bi, Tl, Pb, or Hg, R = Ca, and with an appropriate E = Sr or Ba (such as $Bi_2Sr_2Ca_2Cu_3O_{10}$); and (iii) A–12(*n*–1)*n*–E with A = Tl, Hg, Au, (Cu,C), B, Al, or Ga, R = Ca, and with an appropriate E = Ba or Sr (such as $TlBa_2Ca_2Cu_3O_9$). Studies of these compounds reveal that layers in these compounds can be grouped into two (*3*), namely the charge-reservoir block of (EO)(AO)···(AO)(EO), and the active block of ($CuO_2$)(R)($CuO_2$)···(R)($CuO_2$). The charge-reservoir block provides the sources of charge-carriers for the active block which is considered the main component for the superconductivity in the compound. New high-temperature superconductor families would help further unravel the roles of the charge-reservoir block, the active block, or both.

The record $T_c$ of high-temperature superconducting compounds is 134 K at ambient pressure (*4*) or 164 K at 30 GPa (*5*). Unfortunately, those with a $T_c$ above 120 K contain volatile toxic elements such as Tl in Tl-2223-Ba, which superconducts at 125 K, and Hg in Hg-1223-Ba, which becomes superconducting at 134 K. This poses serious challenges to practical applications. Consequently (*6*), Cu-1212-Ba (or Y-123) remains the most viable material for high-temperature superconducting thin-film devices, in spite of its lower $T_c$ of 93 K; and Bi-2212-Sr and Bi-2223-Sr for high-temperature superconducting conductors, operated at temperatures preferably below 77 K because of their weak flux pinning force. We report a new superconducting system, the interstitially doped $Ba_2Ca_{n-1}Cu_nO_x$ [02(*n*–1)*n*–Ba], which is synthesized under pressure and displays a $T_c$ of 126 K for $n$ = 3 or 117 K for $n$ = 4. The 02(*n*–1)*n*–Ba compound system without C-inclusion exhibits a body-centered tetragonal I4 symmetry and a rather open charge-reservoir block, which offers new flexibility in modifying the compound. For instance, intercalation of carbonate, hydroxyl, or both ions into the charge-reservoir block transforms the 126 K phase into a more stable 90 K phase.

We searched for high-$T_c$ compounds without volatile toxic elements by modifying the charge-reservoir block. Our examination of the existing $T_c$ data reveals a simple empirical rule (*7*) that compounds with simpler charge-reservoir blocks, compounds whose charge-reservoir block contains Ba instead of Sr, and compounds without rare-earth elements, usually have a higher $T_c$. For instance, $YBa_2Cu_3O_7$ displays a $T_c$ ~ 93 K, in contrast to $YBa_2Cu_4O_8$, which has a more complex charge-reservoir block and shows a lower $T_c$ ~ 80 K and to $YSr_2Cu_3O_7$, which has two (SrO) layers in its charge-reservoir block and shows a lower $T_c$ < 60 K. A simpler charge reservoir may be an easier way to retain the integrity of and to improve the coupling between the $CuO_2$ layers in the active block. The higher $T_c$ for compounds with double BaO layers than with double SrO layers may be associated with the higher polarizability of Ba than Sr or the less possible mixing of Ba in the charge-reservoir block with Ca in the active block. The Ba-based perovskite ferroelectrics also often have a higher Curie point, below which polarization appears, than the Sr-based ones. Therefore, a desirable candidate for a high $T_c$ without any volatile toxic element appears to be the Ba-based compound system $Ba_2Ca_{n-1}Cu_nO_x$ [02(*n*–1)*n*–Ba]. This compound system in its ideal form consists of a simple [(BaO)(BaO)] charge reservoir without any (AO) layers and an active block of $n$ ($CuO_2$) layers separated by ($n$–1) Ca layers and is expected to display a body-centered tetragonal I4 symmetry. Compounds with similar structure were observed previously in the nonsuperconducting (PbBa)(YSr)$Cu_3O_8$ [or 0223-(PbBa) with R = (YSr)] (*8*) and the superconducting system $Sr_2Ca_{n-1}Cu_nO_{2n+2}$ [02(*n*–1)*n*–Sr] with a $T_c$ up to ~ 85 K (*9*). The Ba-Ca-Cu-O system has also been studied previously by several groups (*10*–*17*) and was found to form the C-stabilized $(Cu_{1-y}C_y)Ba_2Ca_{n-1}Cu_nO_x$ [(Cu,C)–12(*n*–1)*n*–Ba]

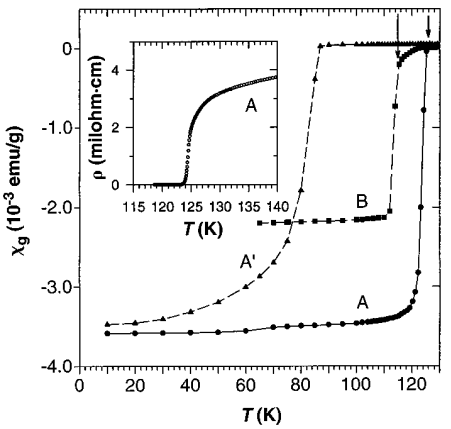


**Fig. 1.** Field-cooled $\chi(T)$ for A samples (0223-Ba) and a B sample (0234-Ba) as synthesized (A and B) and after exposure to humid air (A′). Inset: $\rho(T)$; emu indicates electromagnetic units.

C. W. Chu, Y. Y. Xue, L. Gao, Y. Cao, Texas Center for Superconductivity and Department of Physics, University of Houston, Houston, TX 77204–5932, USA.
Z. L. Du, Y. Y. Sun, N. L. Wu, I. Rusakova, K. Ross, Texas Center for Superconductivity, University of Houston, Houston, TX 77204–5932, USA.
*To whom correspondence should be addressed. E-mail: cwchu@uh.edu
†On leave from National Taiwan University.